TESSERAL RESONANCE OVERLAP INCLUDING THE EFFECTS OF LUNI-SOLAR PERTURBATIONS

Todd. A. Ely* and Kathleen C. Howell†
Purdue University, West Lafayette, IN 47907

Abstract

Eccentric and inclined resonant orbits exhibit complex motions that have the potential to become chaotic. Furthermore, these complex motions may also destabilize classical control strategies. Understanding the mechanisms that cause such motions to occur is crucial to arriving at robust, stable control methods. Previous research has determined that the interaction between resonant tesseral harmonics can produce chaotic responses in the semi-major axis and stroboscopic mean node (primary variables of interest in East-West stationkeeping) of an orbit. However, the previous work did not include the effects of potentially significant luni-solar perturbations; the present effort does so. Utilizing a variety of techniques, including resonance overlap criteria, Poincaré sections, stroboscopic plots, and Lie perturbation methods, resonance overlap is found between interacting lunar harmonics. This overlap result can produce significant excursions in eccentricity. Furthermore, the potential for diffusion between the eccentricity (or inclination) and semi-major axis exists because of the coupling introduced by the tesseral harmonics. However, it is found that the interaction between these two modes (motion in eccentricity and motion in semi-major axis) is slight for orbits with periods of 12 hr or lower. It is concluded that the *qualitative* motion of the semi-major axis and the node, on time scales of interest for mission planning, evolves primarily from tesseral harmonic effects.

Introduction

Satellite orbits that are eccentric and inclined with near-repeating ground tracks can exhibit complex dynamical motions. Of particular interest is the behavior of the semi-major axis and the stroboscopic mean node; controlling these variables is crucial to maintaining a repeat groundtrack. Ely and Howell[1,2] examined the effects of interacting tesseral harmonics on these variables. Depending on the selected mean motion commensurability (i.e., orbits with a 24 hr period, 12 hr period, etc.), inclination, and eccentricity, the interaction can produce a variety of motions ranging between periodic, quasiperiodic, and chaotic. However, the previous work did not include the potentially significant effects of luni-solar perturbations. The current study incorporates these additional gravity terms in the dynamical model so that their impact on the motion (primarily semi-major axis and node) can be determined. Secular perturbation theory is used to determine isolated resonance characteristics (for all the contributing perturbations), and resonance overlap criteria is applied to determine the likelihood of resonance interaction and the potential for chaotic motion.[3] The numerical analysis employs a combination of stroboscopic plots and Poincaré sections. The stroboscopic plots are used to determine the likelihood of extremely long time scale diffusion processes in the fully dimensional system (including all geopotential and luni-solar perturbations with only secular and long-period perturbing terms). Using suitably reduced 2 Degree-of-Freedom (2-DOF) models, the motion can be analyzed using Poincaré sections. The reduction to 2-DOF is accomplished using a combination of first order averaging and second order Lie perturbation methods. A 2-DOF system removes diffusion as a possible type of motion with the resulting model well suited for assessing the existence of regular and/or chaotic motions. The focus of ongoing work is the development of analytical tools for assessing quasiperiodicity and chaos (from resonance overlap and/or diffusion) in the system with coupled geopotential and luni-solar perturbations.

Development of the Dynamical Model

This study considers eccentric and inclined orbits that are *nearly resonant* (or *nearly commensurate*) with the Earth's rotation rate (i.e., orbital periods near 12 hrs). Of primary interest is the long term evolution of these orbits, hence, perturbation expansion terms possessing secular and long period behaviors are retained in the dynamical model. For the time scales of interest, short period effects have little net effect on the long term response. More formally, short period terms are removed by transforming coordinates to a mean element set. The most significant perturbations to a nominal

---

* Graduate Student, School of Aeronautics and Astronautics, Member AIAA, Member AAS

† Associate Professor, School of Aeronautics and Astronautics, Senior Member AIAA, Member AAS

Keplerian orbit in the class being considered include: Earth geopotential (tesseral and zonal) effects and third body effects from the Sun and the Moon.

Model

The dynamical model can be represented formally as an integrable Hamiltonian $H_o(I)$ being perturbed by additional conservative terms $\varepsilon H_1(I,\theta)$. The Hamiltonian is transformed into a set of action/angle variables (I,θ) that prove convenient for studying mean motion resonances with the Earth.[4] Included in H_o is the inverse square gravity term, a secular term due to the Earth's oblateness (i.e., the potential energy term $V_{\mathcal{OB}}$), and an additional term introduced because the reference frame is fixed in the Earth and rotates with it. The perturbation $\varepsilon H_1(I,\theta)$ includes long period potential energy terms from the Earth's tesseral harmonics (longitude dependent) $V_{\mathcal{7}}$, the Earth's zonal harmonics (longitude independent) $V_{\mathcal{Z}}$, the Moon's harmonics $V_{\mathcal{L}}$, and the Sun's harmonics $V_{\mathcal{S}}$. Note, the subscript $\mathcal{OB}$ is used when referring to Earth oblateness, $\mathcal{7}$ for tesseral terms, $\mathcal{Z}$ for zonal terms, $\mathcal{L}$ for lunar quantities, and $\mathcal{S}$ for solar quantities. Formally, the Hamiltonian takes the following form,

$$H = H_o(I) + \varepsilon H_1(I,\theta), \tag{1}$$

$$\begin{aligned} H = &-\frac{s_o^2\mu^2}{2I_1^2} - \dot{\theta}_e I_1 + V_{\mathcal{OB}}(I_1,I_2,I_3) + \\ &\sum V_{\mathcal{7}}(I_1,I_2,I_3,\lambda,\omega) + \sum V_{\mathcal{Z}}(I_1,I_2,I_3,\omega) + \\ &\sum V_{\mathcal{L}}(I_1,I_2,I_3,\omega,\Omega,\Omega_{\mathcal{L}}) + \sum V_{\mathcal{S}}(I_1,I_2,I_3,\omega,\Omega), \end{aligned} \tag{2}$$

where the action/angle pairs are defined as follows,

$$\begin{aligned} &I_1 = s_o L = s_o\sqrt{\mu a}, \quad \lambda = \frac{1}{s_o}(M+\omega) - (\theta_e - \Omega); \\ &I_2 = L\sqrt{1-e^2} - L, \quad \omega; \\ &I_3 = L\sqrt{1-e^2}\cos i - s_o L, \quad \Omega. \end{aligned} \tag{3}$$

Additionally, (a,e,i,M,ω,Ω) are the classical orbital elements, s_o is the integer nearest the ratio: satellite mean motion over Earth rotation rate, μ is the Earth's reduced mass, θ_e is the Greenwich sidereal angle and $\dot{\theta}_e$ is its associated rate, and $\Omega_{\mathcal{L}}$ is the longitude of the ascending node (referenced to the ecliptic plane) of the lunar orbit. Note that the angle λ, called the stroboscopic mean node, has a slow variation in time due to the commensurability between satellite mean motion and the Earth's rotation rate. Furthermore, the perigee ω and the right ascension of the ascending node Ω vary slowly, primarily because of Earth's oblateness. The ascending node of the lunar orbit $\Omega_{\mathcal{L}}$ varies linearly with time.

Tesseral and Zonal Perturbations

The secular and long period geopotential (tesseral and zonal) terms are determined by averaging the geopotential expansion, expressed in terms of classical orbital elements, over the satellite mean anomaly. A brief review of the development follows.[4] The secular oblateness term that remains after averaging is of first order $O(J_2)$ and has the form,

$$V_{\mathcal{OB}} = -\frac{\mu R_e^2 J_2}{a^3(1-e^2)^{3/2}}\left\{\frac{3}{4}\cos^2 i - \frac{1}{4}\right\}. \tag{4}$$

The tesseral terms that remain after averaging are of second order and have the following form,

$$\sum V_{\mathcal{7}} = \sum_{l=2}^{\infty}\sum_{m=1}^{l}\sum_{p=0}^{l}\sum_{q=-\infty}^{\infty} h^{\mathcal{7}}_{lmpq}(a,e,i)\cos[m(\lambda - \lambda_{lm}) - q\omega], \tag{5}$$

where,

$$h^{\mathcal{7}}_{lmpq} = -\frac{\mu R_e^l}{a^{l+1}} F_{lmp}(i) G_{lpq}(e) J_{lm},$$

and R_e is the Earth's radius; $F_{lmp}(i)$ and $G_{lpq}(e)$ are the inclination and eccentricity functions, respectively, defined in Kaula;[8] and $J_{lm} = \sqrt{C_{lm}^2 + S_{lm}^2}$ is the unnormalized coefficient corresponding to the tesseral harmonic of degree l and order m. The eccentricity function $G_{lpq}(e)$ is implemented using a quickly convergent expansion that is well suited for mean motion dynamics.[9] The terms included in the summation satisfy the long period constraint equation $l - 2p + q - m/s_o = 0$. For purposes of simulation, the summation in Eq. (5) is truncated to have finite l and q. Previous analysis[1] has suggested that a minimal set consisting of the largest harmonic and its next largest neighbors is sufficient for determining the qualitative nature of the motion. The current study includes a larger set of harmonics to verify this claim. The value of the phasing angle associated with J_{lm} is computed as follows,

$$\lambda_{lm} = \begin{cases} \frac{1}{m}\tan^{-1}\left(\frac{S_{lm}}{C_{lm}}\right) & l-m \text{ even} \\ \frac{1}{m}\tan^{-1}\left(\frac{C_{lm}}{-S_{lm}}\right) & l-m \text{ odd} \end{cases} \quad (6)$$

The zonal terms $V_{\mathfrak{z}}$ (not including the first order secular oblateness term) that remain in the geopotential expansion after averaging are of second order and have the same representation as Eq. (5) with the following changes: the summation now consists of elements that satisfy $l \geq 3$, $m = 0$, and the constraint equation $q = 2p - l$. Additionally, the zonal harmonic coefficient is defined as $J_l \equiv |C_{l0}|$ and replaces J_{lm} in Eq. (5). The phasing angle λ_l replaces λ_{lm} and is determined as indicated.

$$\lambda_l = \begin{cases} 0 & C_{l0} > 0, l \text{ even} \\ \frac{\pi}{2} & C_{l0} > 0, l \text{ odd} \\ \pi & C_{l0} < 0, l \text{ even} \\ \frac{3\pi}{2} & C_{l0} < 0, l \text{ odd} \end{cases} \quad (7)$$

where the angle argument of the cosine function now takes the form $\lambda_l - q\omega$. As with the tesseral harmonics, the summation is truncated to finite l for simulation purposes. Finally, an additional second order oblateness term $V_{J_2^2}$ must be considered as well. It is represented by,

$$V_{J_2^2} = -\frac{\mu}{a^5}\frac{R_e^4 J_2^2}{4}\left[A(a,e,i)\cos 2\omega + B(a,e,i)\right]. \quad (8)$$

and is included in the summation $\sum V_{\mathfrak{z}}$. The detailed expressions for A and B are discussed by Hough[5] and Delhaise[6]. Ely and Howell[1,2] have shown that the tesseral resonances overlap at most inclinations and eccentricities when a satellite's mean motion is commensurate with the Earth's rotation rate. Trajectories in these overlap regions can be either regular or chaotic depending on the selected initial conditions. Furthermore, at critical inclination an additional resonance from the long period zonal harmonics can overlap with the tesseral harmonics and produce a region of chaos isolated near the separatrices of the primary resonances. A preliminary study by Ely and Howell[4] examined the effect of these resonance interactions on East-West stationkeeping, and suggested that complex motions (high order quasiperiodicity and chaos) can destabilize a classical control technique. To complete the analysis of stable East-West control strategies, it is necessary to assess the impact of luni-solar perturbations on the semi-major axis and stroboscopic node in the resonant regions.

Luni-Solar Perturbations

Third body perturbations from the Sun and the Moon can have a significant impact on high-Earth orbits (HEO). For a satellite in an eccentric HEO at apogee (i.e., $r_a = a(1+e)$), the altitude above the Earth can become significant with a correspondingly low velocity, and, thus, the attraction of the third body becomes large relative to the other perturbations. Indeed, the luni-solar perturbations become $O(J_2)$ for a 24 hr satellite. Consistent with the development of the potential function for third body perturbations that is discussed in Delhaise and Morbidelli,[7] a useful model that is amenable to DOF reduction, yet still retains the essential long period perturbative effects due to the Sun and the Moon, can be obtained. It is based on the following simplifying assumptions:

1. The lunar orbital parameters are defined relative to the ecliptic plane in a coordinate frame centered at the Earth. In this frame, the inclination $i_{\mathfrak{L}}$ and semi-major axis $a_{\mathfrak{L}}$ of the lunar orbit are approximately constant, while the longitude of the ascending node varies linearly with time $\Omega_{\mathfrak{L}} = \dot{\Omega}_{\mathfrak{L}} t + \Omega_{\mathfrak{L}_0}$.
2. The orbital parameters associated with the solar 'orbit' are defined with respect to the equatorial plane in a coordinate frame centered at the Earth. In this frame, the Sun appears to orbit the Earth in the ecliptic plane, and the relative motion is denoted the 'apparent orbit' of the Sun. The inclination $i_{\mathfrak{S}}$ (which equals the obliquity of the ecliptic ε, the angle between the equatorial and ecliptic planes) and semi-major axis $a_{\mathfrak{S}}$ of the solar 'orbit' are approximately constant. Additionally, the longitude of the ascending node $\Omega_{\mathfrak{S}}$ can be assumed constant for the time scales of interest.
3. The eccentricity of the lunar and solar orbits are assumed as zero.
4. The Hamiltonian is averaged over the satellite mean anomaly up to first order.
5. The Hamiltonian is averaged over the Moon and the Sun's mean anomaly in their respective orbits up to first order.

Incorporating these assumptions results in a lunar contribution to the Hamiltonian that can be written in the following form,

$$\sum V_{\mathcal{L}} = \sum_{\substack{l=2,\\ l\ \text{even}}}^{\infty} \sum_{m=0}^{l} \sum_{s=0}^{l} \sum_{p=0}^{l} h^{\mathcal{L}}_{lmsp}(a,e,i,a_{\mathcal{L}},i_{\mathcal{L}})(-1)^{k_2} \times \left\{ U_l^{m,-s}(\varepsilon)\cos(m_+ \cdot \theta) + U_l^{m,-s}(\varepsilon)\cos(m_- \cdot \theta) \right\}, \tag{9}$$

where,

$$h^{\mathcal{L}}_{lmsp} = -\mu_{\mathcal{L}}(-1)^{k_1} \frac{\varepsilon_m \varepsilon_s (l-s)!}{2a_{\mathcal{L}}(l+m)!} \left(\frac{a}{a_{\mathcal{L}}}\right)^l \times F_{lmp}(i) F_{ls(l/2)}(i_{\mathcal{L}}) H_{lp(2p-l)}(e),$$

$$\varepsilon_m = \begin{cases} 1 \text{ if } m = 0, \\ 2 \text{ if } m \neq 0, \end{cases} \quad \varepsilon_s = \begin{cases} 1 \text{ if } s = 0, \\ 2 \text{ if } s \neq 0, \end{cases}$$

$k_1 = \left\| \frac{m}{2} \right\|$, the largest integer part of $\frac{m}{2}$,

$k_2 = m + s$,

$b_s = 0$ if s even and $b_s = 1/2$ if s is odd,

and, finally,

$$(m_{\pm} \cdot \theta) = \left((l-2p)\omega + m\Omega \pm s(\Omega_{\mathcal{L}} - \pi/2) - b_s\pi\right).$$

Details associated with the function $U_l^{m,s}(\varepsilon)$ can be found in Delhaise and Morbidelli;[7] $F_{ijk}(\cdot)$ is the inclination function defined in Kaula;[8] and $H_{lp(2p-l)}(e)$ is an eccentricity function similar to $G_{lpq}(e)$.[9] Note that the expression for the lunar potential is complicated by the fact that a frame rotation is required to obtain orbital elements that are referred to the ecliptic plane. Since the expression for the solar potential does not require this rotation it has a representation that is simpler than the lunar contribution, that is,

$$\sum V_{\mathcal{S}} = \sum_{\substack{l=2,\\ l\ \text{even}}}^{\infty} \sum_{m=0}^{l} \sum_{s=0}^{l} \sum_{p=0}^{l} h^{\mathcal{S}}_{lmsp}(a,e,i,a_{\mathcal{S}},i_{\mathcal{S}}) \times \cos\left[(l-2p)\omega + m(\Omega - \Omega_{\mathcal{S}})\right], \tag{10}$$

where,

$$h^{\mathcal{S}}_{lmsp} = -k_m \frac{\mu_{\mathcal{S}}}{a_{\mathcal{S}}} \frac{(l-m)!}{(l+m)!} \left(\frac{a}{a_{\mathcal{S}}}\right)^l \times F_{lmp}(i) F_{lms}(i_{\mathcal{S}}) H_{lp(2p-l)}(e),$$

$$k_m = \begin{cases} 1, & m = 0 \\ 2, & m \neq 0 \end{cases},$$

and, the definitions for the inclination and eccentricity functions are of the same functional form as those corresponding to the lunar contribution. The luni-solar perturbations, in their present forms, increase the system's phase space dimension from 4 to 6 (i.e., 3-DOF) and renders it nonautonomous. Of particular note is the independence of Eqs. (9) and (10) from the stroboscopic mean node; hence, the impact of these perturbations on the action I_1 ($\Rightarrow a$) is indirect.

Reduction to 2 Degrees-of-Freedom

For the class of resonances considered in this study, Eq. (2) embodies the essential secular and long period effects that govern an orbit's long term evolution. However, the system is still not in a form convenient for analysis using Poincaré sections; reduction to a 2-DOF system is required. In particular, it is desirable to remove the dependence on the three quantities representing the longitude of the ascending node that appear in Eqs. (9) and (10): Ω, $\Omega_{\mathcal{L}}$, and $\Omega_{\mathcal{S}}$. This will result in (I_1, λ) and (I_2, ω) as the independent action/angle pairs. The ascending node of the satellite orbit Ω varies nonlinearly because of the coupling between terms in the Hamiltonian, but, is secular in the regions of interest. The ascending node of the lunar orbit $\Omega_{\mathcal{L}}$ is linear and is the source of the Hamiltonian's explicit time dependence. Finally, the ascending node of the solar orbit $\Omega_{\mathcal{S}}$ can be approximated as a constant over the time scales of interest. The reduction to 2-DOF must be accomplished carefully for two reasons: the luni-solar perturbations can become first order $O(J_2)$ for large semi-major axes and the potential for additional resonances beyond those examined thus far (i.e., mean motion and critical inclination resonances) may be introduced.

Assessment of Order

Regarding the first issue, i.e., the asymptotic order of the luni-solar perturbations, it can be shown that for 24 hr orbits, the luni-solar perturbations in Eqs. (9) and (10) are of the same order as the secular oblateness term in Eq. (4), that is,

$$O\left\{\frac{\mu_L}{a_L}\left(\frac{a}{a_L}\right)^2\right\} \sim O\left\{\frac{\mu}{a}\left(\frac{R_e}{a}\right)^2 J_2\right\}. \qquad (11)$$

The tesseral and zonal harmonics maintain their contribution as second order effects. As the semi-major axis is decreased, the luni-solar perturbations increase their order incrementally from first towards second order. That is, they introduce an undetermined gauge $0 < \delta \le 1$ in their order representation, i.e., $O(J_2^{1+\delta})$. For an analytical reduction procedure, it is desirable to use a first order secular approximation for the longitude of ascending node Ω. In the 24 hr case, the combined effects of oblateness and luni-solar perturbations prevent a first order secular approximation from being valid. A semi-analytical reduction would be required. For resonances with a shorter period, such as the 12 hr case, the first order secular approximation is valid, but the reduction should be accomplished to the second order. In these cases, it is advantageous to use a Lie perturbation method, since this technique yields the desired transformations without the need for any inversion of implicit functions (which is the case with standard canonical perturbation theory).

Lie Perturbation Analysis

Before addressing the issue of additional resonances between ω, Ω, and Ω_L, the perturbation analysis will be accomplished. To first order, the method is equivalent to an approach involving standard canonical perturbation theory, however to second order the algorithms differ in their implementation because the Lie method does not use mixed generating functions. It utilizes a determining function $W(\bar{I},\bar{\theta},\varepsilon)$ that is a function of the transformed variables, indicated by the bar. The relationship between the new action/angle pairs $(\bar{I},\bar{\theta})$ and the old action/angle pairs (I,θ) is obtained formally by applying Hamilton's equations to $W(\bar{I},\bar{\theta},\varepsilon)$, where the determining function replaces the Hamiltonian and the small parameter ε replaces time. For autonomous systems Hori[10] obtained a perturbation series that eliminates dependence on selected angles, i.e., Ω and Ω_L. The resulting perturbation equations written to second order are,

$$\begin{aligned}
&0: \quad \bar{H}_0(\bar{I},\bar{\theta}) = H_0(\bar{I}),\\
&1: \quad \bar{H}_1(\bar{I},\bar{\theta}) = \left\langle H_1(\bar{I},\bar{\theta})\right\rangle,\\
&\qquad \tilde{H}_1(\bar{I},\bar{\theta}) \equiv H_1(\bar{I},\bar{\theta}) - \left\langle H_1(\bar{I},\bar{\theta})\right\rangle,\\
&\qquad \left[H_0(\bar{I}), W_1(\bar{I},\bar{\theta})\right] = \tilde{H}(\bar{I},\bar{\theta}),\\
&2: \quad \bar{H}_2(\bar{I},\bar{\theta}) = \left\langle H_2(\bar{I},\bar{\theta})\right\rangle - \frac{1}{2}\left\langle\left[\tilde{H}(\bar{I},\bar{\theta}), W_1(\bar{I},\bar{\theta})\right]\right\rangle,
\end{aligned} \qquad (12)$$

where $\bar{H}_i$ is the transformed Hamiltonian, W_i is an element of $W = \sum_{i=1}^{\infty} \varepsilon^i W_i$, the index i is the associated order, $[\cdot,\cdot]$ is a Poisson bracket, and $\langle\rangle$ is the averaging operation over the selected angles (i.e., Ω, Ω_L). It is noteworthy that the second order Hamiltonian does not require the second order determining function. Now, apply Eqs. (12) to the system in Eq. (2) with $H_0 = -s_0^2\mu^2/2I_1^2 - \dot{\theta}_e I_1 + V_{08} + \dot{\Omega}_L I_4$ (I_4 is introduced to make the system autonomous), $H_1 = \sum V_L + V_S$, and $H_2 = \sum V_7 + V_3$. The zeroth order result simply returns the original Hamiltonian with the new actions replacing the old ones. The result for the first order Hamiltonian is typical, too. The computation yields,

$$\begin{aligned}
\bar{H}_1 = &\sum_{m,s=0} h^L_{lmsp}(\bar{I}_1,\bar{I}_2,\bar{I}_3) U_l^{0,0} \cos[(l-2p)\bar{\omega}] +\\
&\sum_{m,s=0} h^S_{lmsp}(\bar{I}_1,\bar{I}_2,\bar{I}_3) \cos[(l-2p)\bar{\omega}].
\end{aligned} \qquad (13)$$

For simplicity, the remaining results show only the lunar contribution, since results for the solar contribution are similar. The expression for the first order term of the determining function W_1 has the form,

$$\begin{aligned}
W_1 = -\sum_{m,s\neq 0} \Bigg\{ &\frac{(-1)^{k_2} h^L_{lmsp} U_l^{m,-s}}{m_+ \cdot \dot{\bar{\theta}}} \sin(m_+ \cdot \bar{\theta}) +\\
&\frac{(-1)^{k_2} h^L_{lmsp} U_l^{m,+s}}{m_- \cdot \dot{\bar{\theta}}} \sin(m_- \cdot \bar{\theta}) \Bigg\}.
\end{aligned} \qquad (14)$$

The computation for the second order term in the expression for the Hamiltonian is tedious, but straightforward. The Poisson bracket that appears in the expression for $\bar{H}_2$ is evaluated with the following result,

$$\begin{aligned}
\left\langle\left[\tilde{H}_1, W_1\right]\right\rangle = &\sum_{\alpha=2}^{\infty}\sum_{\beta=0}^{\alpha}\sum_{l=2}^{\infty}\sum_{p=0}^{l}\sum_{m=1}^{r}\sum_{s=1}^{r}\left(D_+^L + D_-^L\right)\times\\
&\cos\left\{\left[(\alpha-2\beta)-(l-2p)\right]\bar{\omega}\right\},
\end{aligned} \qquad (15)$$

where $r = \min(\alpha, l)$ and,

$$D_{\bar{z}}^{\bar{z}} = \frac{\left(U_l^{m,\pm s}\right)^2}{2}\left[\frac{h_{lmsp}^{\bar{z}}}{m_{\pm}\cdot\bar{\theta}}\left((l-2p)\frac{\partial h_{\bar{\alpha}ms\beta}^{\bar{z}}}{\partial \bar{I}_2}+m\frac{\partial h_{\bar{\alpha}ms\beta}^{\bar{z}}}{\partial \bar{I}_3}\right)+ h_{\bar{\alpha}ms\beta}^{\bar{z}}\left((\alpha-2\beta)\frac{\partial}{\partial \bar{I}_2}\left(\frac{h_{lmsp}^{\bar{z}}}{m_{\pm}\cdot\bar{\theta}}\right)+m\frac{\partial}{\partial \bar{I}_3}\left(\frac{h_{lmsp}^{\bar{z}}}{m_{\pm}\cdot\bar{\theta}}\right)\right)\right]. \tag{16}$$

The remaining part of the second order term $\overline{H}_2$ is comprised simply of the zonal and tesseral terms with the old action/angles replaced by the new, that is $\langle H_2\rangle = \Sigma V_7(\bar{I},\bar{\theta}) + V_3(\bar{I},\bar{\theta})$. Assembling the preceding Hamiltonian terms produces,

$$\overline{H} = \overline{H}_0 + \overline{H}_1 + \overline{H}_2, \tag{17}$$

where this is a system with 2-DOF; $(\bar{I}_1,\bar{\lambda})$ and $(\bar{I}_2,\bar{\omega})$ are the participating action/angle pairs; and $\bar{I}_3$ and $\bar{I}_4$ are constants of motion. Note, for ease of notation the overbars on the action/angle variables are dropped in the sequel. The luni-solar and zonal terms are dependent on perigee only, and produce a primary resonance at critical inclination. Each tesseral harmonic produces its own resonance that can interact with the other tesserals and, near the critical inclination, with the resonance produced by the luni-solar and zonal perturbations. As observed by Delhaise and Morbidelli[7], inclusion of luni-solar terms, beyond just the zonal terms in the Hamiltonian, increases the magnitude of resonant harmonic terms significantly at critical inclination. This results in a significant increase in the resonant action excursions (functions of eccentricity and inclination) and a corresponding decrease in perigee's libration period. However, this does not provide the complete picture, additional resonances exist that must be considered before $\overline{H}$ can be used to study selected orbits.

Lunar Resonances

The presence of additional resonances between ω, Ω, and $\Omega_{\mathcal{L}}$ and their impact on tesseral resonances must be considered before proceeding with the analysis of $\overline{H}$, i.e., Eq. (17). Resonance between these angles is defined as the existence of linear combinations of angular frequencies that yield $m_{\pm}\cdot\dot{\theta} = (l-2p)\dot{\omega} + m\dot{\Omega} \pm s\dot{\Omega}_{\mathcal{L}} \approx 0$. Delhaise and Morbidelli[7] investigate the existence of resonances of the form $m\dot{\Omega} \pm s\dot{\Omega}_{\mathcal{L}} \approx 0$, for orbits at the critical inclination, and found none of any significant order. Expanding the search to include $i < 70°$ and $e < 1$ the resonance $((l-2p), m, \pm s) = (0,1,-1)$ does exist for $e < .44$ and $58° < i < 70°$. If the search for resonances is expanded further, to include $l - 2p \neq 0$, a greater array of resonances are encountered. Note that the index l is set equal to two so that the search for primary resonances can be restricted to the lowest orders. Figure 1 depicts the locations of these resonances as functions of eccentricity and inclination. In the figure, there are five families of curves emanating from an eccentricity of one. The straight line at each center corresponds to the resonance with $s = 0$; curves to either side correspond to $s \in \{1, 2\}$. Two families are labeled, the family at critical inclination, $(2,0,\pm s)$, and a neighbor at inclination of 69°, $(2,1,\pm s)$. Within these two families, the resonance that is present when $s = 0$ is highlighted by the thicker line. Using secular perturbation theory, a primary effect of an isolated resonant term is to increase the amplitude of oscillation for a system's action by a fractional order. For example, if an isolated lunar harmonic term has order $O(J_2^{1+\delta})$, then the amplitude of oscillation in deep resonance is $O(J_2^{(1+\delta)/2})$, recall δ is currently an unknown gauge. As conditions depart from deep resonance the amplitude approaches $O(J_2^{1+\delta})$. However, with other resonances present the potential exists for even larger chaotic excursion in the action variable.[3] Figure 1 suggests, because of the close spacing of resonance locations, that lunar resonances can overlap and produce chaotic responses in eccentricity and

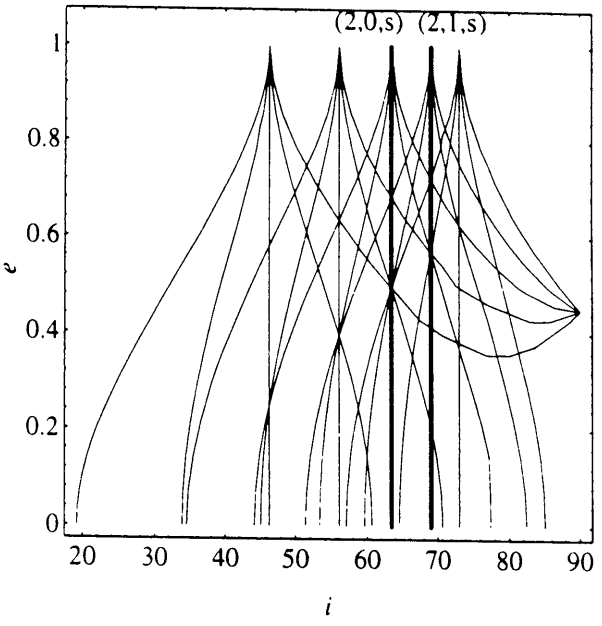

Figure 1: Location of resonance centers of the form $m_1\dot{\omega} + m_2\dot{\Omega} + m_3\dot{\Omega}_{\mathcal{L}} \approx 0$

inclination. Simple first order calculations can yield estimates for the excursions in the actions, and using the resonance overlap criteria (see Lichtenberg and Lieberman[3]), the potential for global chaos (in eccentricity and inclination) can be ascertained.

Consider a Hamiltonian consisting only of the oblateness term Eq. (4) and lunar perturbing terms from Eq. (9),

$$H = V_{\bar{\sigma}\bar{s}}(I_1, I_2, I_3) + \dot{\Omega}_{\mathcal{L}} I_4 + \sum V_{\mathcal{L}}(I_1, I_2, I_3, \omega, \Omega, \Omega_{\mathcal{L}}). \tag{18}$$

In this form I_1 is a constant of motion because the node λ is not present. Consider an isolated resonance. The Hamiltonian then reduces to the oblateness term and a single harmonic,

$$H = V_{\bar{\sigma}\bar{s}}(I_1, I_2, I_3) + \dot{\Omega}_{\mathcal{L}} I_4 + (-1)^{k_2} h^{\mathcal{L}}_{lmsp}(I_1, I_2, I_3) U_l^{m,\mp s}(\varepsilon)\cos(m_{\pm}\cdot\theta). \tag{19}$$

In this form the oblateness term is first order $O(J_2)$ and the harmonic term is of a fractionally higher order $O(J_2^{1+\delta})$. Using the generating function $F_2(\hat{I},\theta) = (m_{\pm}\cdot\theta)\hat{I}_2 + \Omega\hat{I}_3 + \Omega_{\mathcal{L}}\hat{I}_4$ transform to the rest frame of the resonance, where the new actions are indicated by carets (^). Note, the rest frame is determined using $m_{\pm}\cdot\dot{\theta} \approx 0 \Rightarrow (I_1^*, I_2^*, I_3^*, I_4^*)$, and the (*) identifies the actions at exact resonance. Expanding in a Taylor series around this location yields the first order Hamiltonian for this resonance,

$$H = \frac{1}{2}\frac{\partial^2 V_{\bar{\sigma}\bar{s}}}{\partial \hat{I}_2^2}(\Delta\hat{I}_2)^2 + (-1)^{k_2} h^{\mathcal{L}}_{lmsp}(I_1^*, I_2^*, I_3^*) U_l^{m,\mp s}(\varepsilon)\cos(m_{\pm}\cdot\hat{\theta}), \tag{20}$$

where $\Delta\hat{I}_2 = \hat{I}_2 - \hat{I}_2^*$ and,

$$\frac{\partial^2 V_{\bar{\sigma}\bar{s}}}{\partial \hat{I}_2^2} = \frac{3}{2}\frac{J_2 R_e^2}{a^4(1-e^2)^{5/2}}\left((l-2p)^2(2-15\cos^2 i) + 5m(l-2p)\cos i - m^2\right) \tag{21}$$

In this form, the maximum *half-width* excursion in the action is,

$$\Delta\hat{I}_2^{\max} = 2\sqrt{\left| h^{\mathcal{L}}_{lmsp}(I_1^*, I_2^*, I_3^*) U_l^{m,\mp s}(\varepsilon) \Big/ \frac{\partial^2 V_{\bar{\sigma}\bar{s}}}{\partial \hat{I}_2^2}\right|}. \tag{22}$$

and using the first variations of Eqs. (3) with $I_2 = (l-2p)\hat{I}_2$, $I_3 = m\hat{I}_2 + \hat{I}_3$, and $I_4 = \pm s\hat{I}_2 + \hat{I}_4$ the half-width excursions in eccentricity and inclination become,

$$\Delta e^{\max} = \left| -(l-2p)\frac{\sqrt{1-e^2}}{Le}\Delta\hat{I}_2^{\max}\right|, \qquad \Delta i^{\max} = \left|\frac{\Delta e^{\max}}{1-e^2}\left(\frac{m}{(l-2p)\sin i} - e\cot i\right)\right|. \tag{23}$$

As an example consider resonance at critical inclination. This corresponds to $((l-2p), m, \pm s) = (2,0,0) \Rightarrow h^{\mathcal{L}}_{2000}$ and $(-2,0,0) \Rightarrow h^{\mathcal{L}}_{2002}$, and results in four harmonic terms that can be combined into one single term because the angular argument is the same. For a 12 hr orbit at an inclination of 63.4° and .7 eccentricity, the maximum half-width excursions become $\Delta i^{\max} = 3.8°$ and $\Delta e^{\max} = .096$ and perigee's linear period of libration is roughly 9.1 years. As Figure 1 indicates there is an additional resonance nearby at an approximate inclination of 69° (for energy to remain constant the eccentricity is ~.55) corresponding to $(2,1,0) \Rightarrow h^{\mathcal{L}}_{2100}$ and has two terms that can be combined into one. The maximum half-width excursion for this resonance becomes $\Delta i^{\max} = 2.9°$ and $\Delta e^{\max} = .108$. Figure 1 shows that at this inclination and eccentricity, these resonances should overlap, and are likely to produce a region of chaotic motion. To see that this is indeed the case, Poincaré sections for the Hamiltonian in Eq. (18) (with $s = 0$ so that the system has only 2-DOF) are depicted in Figure 2a,b. The selected energy surface is defined by the initial conditions $(a, e, i, M, \omega, \Omega) = (26574 \text{ km}, .7, 64°, -210°, 200°, 0°)$, and other initial conditions on the section are selected using this energy surface. The upper plot, Figure 2a, depicts the section on (ω, e), and the lower plot, Figure 2b, corresponds to (ω, i). Note the horizontal line in the section (ω, e) at $e = .76$ indicates that the eccentricity has become sufficient to produce orbits that are subterranean. Clearly the resonances have overlapped, and there is a large region of chaotic motion surrounding the surviving islands of regular motion near critical inclination. An initial condition lying in the chaotic region can experience an extremely large variation in eccentricity $\Delta e \sim .35$ and inclination $\Delta i \sim 10°$, while a trajectory in the surviving island can incur relatively

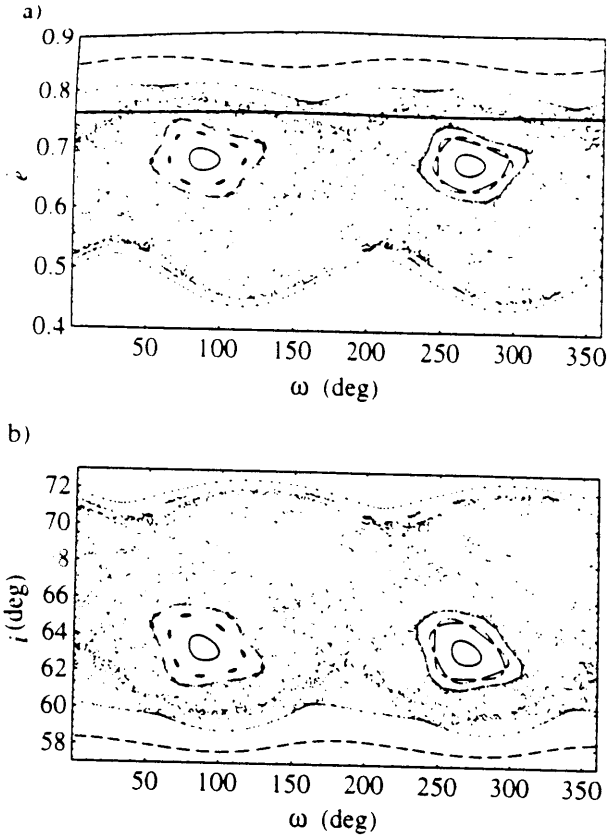

Figure 2a, b: Poincaré sections near the critical inclination with only Lunar perturbations $s = 0$

smaller excursions with maximums of $\Delta e \sim .1$ and $\Delta i \sim 4.5°$. Also, trajectories outside of the chaotic region (see for example $(\omega, i) = (0°, 72°)$) experience more modest excursions. Furthermore, the excursions in eccentricity can be even more dramatic when the additional resonances corresponding to $s \neq 0$ are included in the dynamical model. Coupling the intricate lattice of resonance locations shown in Figure 1 with significant excursions in the action from each resonance suggests the presence of an even larger region of chaotic motion than indicated in Figure 2. Indeed, simulations have shown that the model in Eq. (18) with $l = 2$ (and s *not* restricted to 2) can produce excursions in eccentricity that are larger than $\Delta e \sim .35$. A sample eccentricity history is shown in Figure 3 with associated initial conditions $(a, e, i, M, \omega, \Omega) = (26574$ km, .7, 60.5°, $-210°$, 270°, 0°). The trajectory experiences a shift of .4 in eccentricity. Figure 1 also suggests the interaction

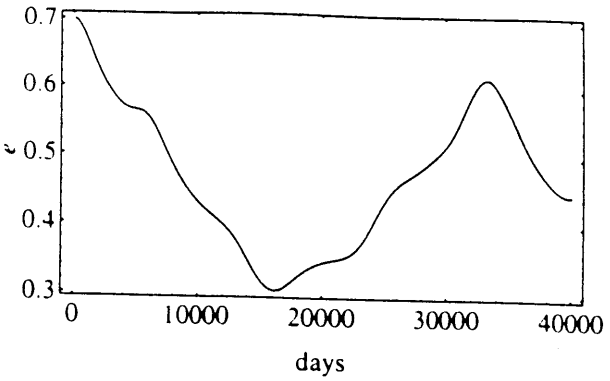

Figure 3: Sample trajectory in chaotic region with only Lunar Perturbations $s \neq 0$

is greater at moderate eccentricities. Clearly, multiple resonance interaction between lunar harmonics is an area that needs more thorough study.

Combined Tesseral and Luni-Solar Resonances

Returning to the issue of the interaction between tesseral harmonics and luni-solar harmonics, the time scale associated with the lunar harmonics is longer (recall, the linear libration period of perigee at critical inclination and .7 eccentricity is ~ 9.1 years) than that of the largest tesseral harmonic (where the linear libration period of $\psi \equiv 2(\lambda - \lambda_{32}) - \omega$, the stationary nodal angle at critical inclination and .7 eccentricity, is ~ 1.4 years). Thus, the system with tesseral, zonal, and luni-solar perturbations is characterized by two time scales, and, in the full non-autonomous 3-DOF model, the actions I_2, I_3, and I_4 are *nearly* asymptotic, adiabatic invariants relative to I_1. However, this multi-dimensional problem introduces complex interactions between resonances that precludes an asymptotic analysis from being accurate over sufficiently long time-scales. Even with weakly interacting resonances (i.e., the interaction between tesserals and luni-solar perturbations is at most $O(J_{lm}) \sim O(J_2^2)$) the actions can diffuse and cause large shifts in their time response.[3] But, diffusion is an extremely long time scale process that may not be significant in the current problem. To ascertain the potential for diffusion, a series of stroboscopic plots are obtained in the (a, ψ) plane for various model effects.

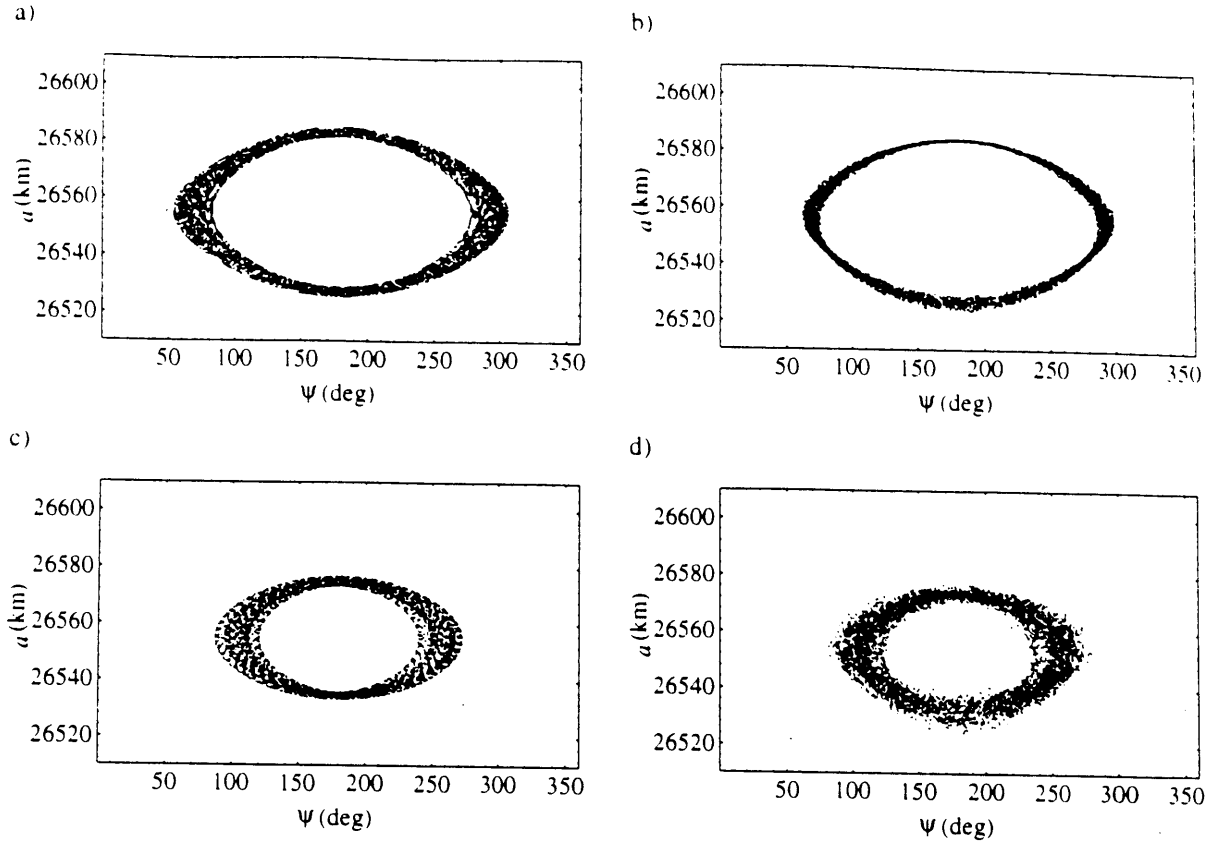

Figure 4a, b, c, d: Stroboscopic plots (500,000 day span sampled every 100 days) illustrating the interaction of perturbations on (a, ψ) and showing the potential for diffusion. For (a) and (b), initial (a, λ) are near separatrix and initial (e,i,ω,Ω) are not in resonance overlap region. For (c) and (d), initial (a, λ) are not near separatrix and initial (e,i,ω,Ω) are in resonance overlap region. The model in (a) and (c) includes only tesseral harmonics, and the model in (b) and (d) includes tesseral, zonal, and luni-solar harmonics.

The data for the stroboscopic plots is obtained by sampling (a, ψ) every 100 days, the nominal length of a trajectory is 500,000 days. As with all the data produced, the veracity of the propagations have been verified by simulations using various numerical integration (4/5 Cash-Karp Runge-Kutta and Bulirsch-Stoer using the modified midpoint method for steps) and symplectic mapping (1st-order Wisdom mapping) schemes. When appropriate, the energy remained constant to machine precision for the duration of the propagation. Figure 4 shows selected results. In Figure 4a,c, the dynamical model includes *only* low order tesseral harmonics through V_{3210}^{7}, all other perturbations beside the secular oblateness are turned off. The model used to generate Figure 4b,d includes the same tesseral harmonics, plus zonal harmonics through $V_{404\pm4}^{3}$, and luni-solar harmonics through $V_{2222}^{4,5}$. The initial conditions selected in Figure 4a,b place (a, ψ) near the separatrix of V_{3210}^{7} and (e,i,ω,Ω) are in the primary island at critical inclination (see Figure 2). The initial conditions in Figure 4c,d place (a, ψ) further from the separatrix of V_{3210}^{7} and (e,i,ω,Ω) are in the chaotic sea (see Figure 2). In the case with only tesseral harmonics, diffusion is not possible, and the trajectories can be confined by KAM surfaces. The stroboscopic plots cannot reveal the KAM surfaces, however they provide information on the possible extent of motion on the (a, ψ) plane. In both Figure 4a,c the motion is confined (i.e. libration) with distinct edges present – indicative of bounding KAM surfaces. When the luni-solar perturbations are present the trajectories can diffuse, however, as shown in Figure 4b,d. The motion remains in libration – no large scale diffusion is present. A case, not shown, with the initial (a, ψ) closer to the separatrix of V_{3210}^{7} did exhibit a trajectory with chaotic transitions from libration to rotation – diffusion enhanced the size of

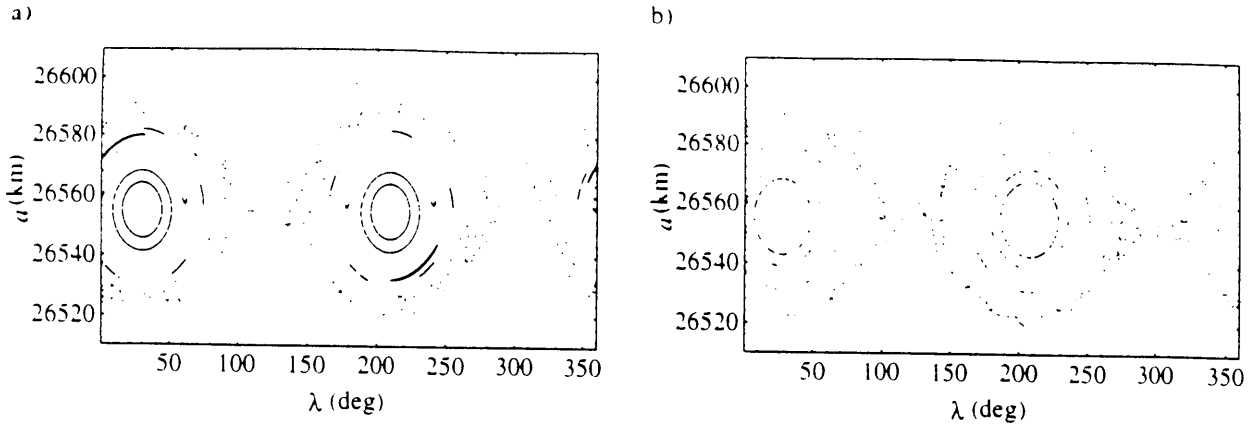

Figure 5a,b: Poincaré section of 12 hr orbit at $i = 55°$, $e = .7$ (nominally), $\omega = 200°$: (a) includes only low order tesserals, (b) includes tesserals, zonals, luni-solar perturbations using Lie perturbation result.

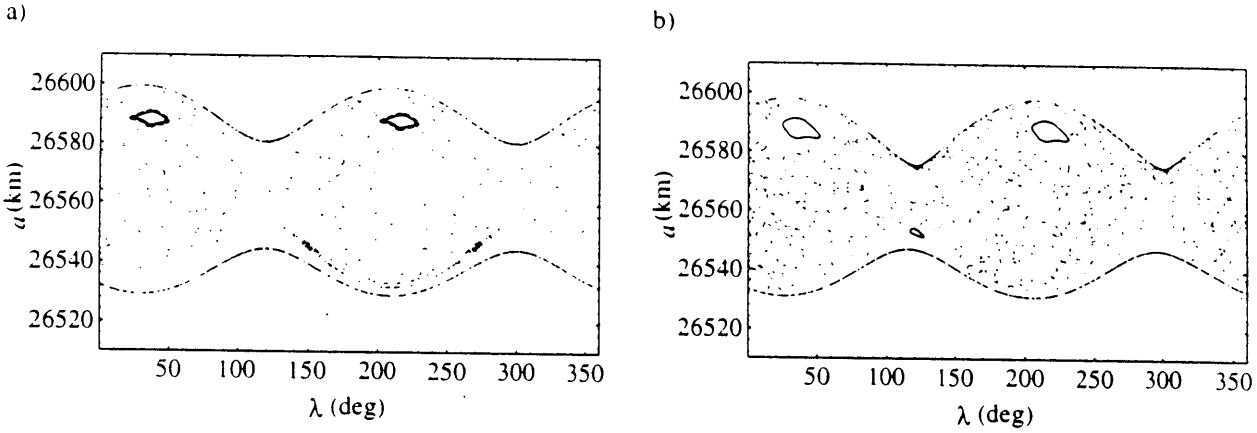

Figure 6a, b: Poincaré section of 12 hr orbit at $i = 23°$, $e = .7$ (nominally), $\omega = 200°$: (a) includes only low order tesserals, (b) includes tesserals, zonals, luni-solar perturbations using Lie perturbation result.

the chaotic region near the separatrix. These results indicate that the addition of zonal and luni-solar perturbations do not affect the motion of (a, ψ) (or (a, λ)) greatly over significant time-scales. Hence, it is reasonable to use the 2-DOF model obtained from the Lie perturbation analysis to assess the impact of luni-solar perturbations on the motion of (a, λ) using Poincaré sections.

Using the 2-DOF model of Eq. (17) to construct Poincaré sections, comparisons with prior results that use a model consisting of only tesseral harmonics can be made. Prior work has shown that as inclination decreases away from the critical value the region of chaos near the separatrix of the primary tesseral resonance grows.[1,2,4] Eventually, at a sufficiently small inclination, the entire region within the separatrix becomes chaotic. This trend is examined in the next set of figures for the 12 hr example at a nominal .7 eccentricity. The model using only tesseral effects, for brevity labeled '*Tesseral*,' includes harmonics through V^7_{3210}. And, the model using Eq. (17), denoted '*All Effects*,' includes tesseral and zonal harmonics through $V^7_{444(\pm 4)}$ and all 1st and 2nd order luni-solar perturbations with $l = 2$. Figure 5a depicts a section for a 12 hr orbit at an inclination of 55° and a nominal .7 eccentricity obtained using the *Tesseral* model. Figure 5b depicts the same conditions using the *All Effects* model. In both cases the region of chaos remains isolated to the separatrix region. However, note that the island structures depicted in Figure 5a have not been duplicated in Figure 5b. Efforts are currently underway to analytically analyze the mechanisms causing the inner islands to appear in Figure 5a and their apparent disappearance in Figure 5b. Now consider the case of a fully developed chaotic region as shown in Figure 6a. Again, the *Tesseral* model is used and the orbit is a 12 hr

case with nominal .7 eccentricity, but now the inclination is 23°. Figure 6b depicts the same conditions using the *All Effects* model. There is little discernible qualitative difference between the two figures. These results demonstrate that the influence of zonal and luni-solar perturbations on the qualitative long-term evolution of semi-major axis and node is small. The largest impact is the disappearance of inner islands in Figure 5b, although this may be due to higher order tesseral harmonics, and not the third body perturbations.

Conclusions

A great variety of resonance phenomena can be encountered by satellite orbits that are eccentric, inclined, and commensurate with the Earth's rotation rate. In particular, the commensurability with the Earth's rotation rate yields tesseral harmonics that can overlap and produce chaotic motions of the semi-major axis. Furthermore, overlapping lunar resonances can result in chaotic motions of eccentricity and inclination. However, the coupling between these two resonance types produces an extremely long time scale diffusion process rather than a strong primary resonance overlap. This implies the semi-major axis and stroboscopic node evolve primarily from the influence of the tesseral harmonics. Current investigations include development of analytical tools to determine the transition from local to global chaos of (a, λ) and development of robust East-West stationkeeping algorithms to control (a, λ).

Acknowledgments

The authors would like to thank Purdue University and the Purdue Research Foundation for their continuing support under a PRF Research Grant.

References

1. Ely, T. A., and Howell, K. C. [1996]. Long Term Evolution of Artificial Satellite Orbits Due to Resonant Tesseral Harmonics. *Journal of the Astronautical Sciences* (to appear).
2. Ely, T. A., and Howell, K. C. [1995]. Resonance Overlap of Tesseral Harmonics in the Artificial Earth Satellite Problem. 1995 SIAM Dynamical Systems Conference, Snowbird, Utah, May 21-24.
3. Lichtenberg, A. J., and Lieberman, M. A. [1992]. *Regular and Chaotic Dynamics*. Springer-Verlag.
4. Ely, T. A., and Howell, K. C. [1995]. Issues Concerning East-West Stationkeeping of Satellite Orbits with Resonant Tesseral Harmonics. Paper No. AAS 95-341, AAS/AIAA Astrodynamics Specialist Conference, Halifax, Nova Scotia, Canada, August 14-17.
5. Hough, M. E. [1979]. *Orbits Near Critical Inclination, Including Luni-Solar Perturbations*. Ph.D. Thesis, Stanford University, Stanford, California.
6. Delhaise, F., and Henrard, J. [1993]. The Problem of Critical Inclination Combined with a Resonance in Mean Motion in Artificial Satellite Theory. *Celestial Mechanics and Dynamical* **55**, 261 - 280.
7. Delhaise, F., and Morbidelli, A. [1993]. Luni-Solar Effects of Geosynchronous Orbits at the Critical Inclination. *Celestial Mechanics and Dynamical Astronomy* **57**, 155-173.
8. Kaula, W. M. [1966]. *Theory of Satellite Geodesy*. Blaisdell.
9. Giacaglia, G. E. O. [1976]. A Note on Hansen's Coefficients in Satellite Theory. *Celestial Mechanics and Dynamical Astronomy* **14**, 515-523.
10. Hori, G. [1966]. Theory of General Perturbations with Unspecified Canonical Variables. *Publications of the Astronomical Society of Japan* **18**, 287-296.